Small-angle neutron-scattering study of micellar structure and interparticle interactions in Triton X-100 solutions

P.S. Goyal,[1] S.V.G. Menon,[2] B.A. Dasannacharya,[1] and P. Thiyagarajan[3]
[1] *Solid State Physics Division, Bhabha Atomic Research Centre, Bombay 400 085, India*
[2] *Theoretical Physics Division, Bhabha Atomic Research Centre, Bombay 400 085, India*
[3] *Intense Pulsed Neuron Source, Argonne National Laboratory, Argonne, Illinois 60439*
(Received 9 August 1994)

Extensive measurements of small-angle neutron-scattering cross sections from the nonionic micellar solutions of Triton X-100 in D_2O are reported. An analysis of data at ambient temperature shows that the micelles are oblate ellipsoids of revolution with an axial ratio around two even at a concentration as low as 1% Triton X-100, and that there are about 20 molecules of D_2O per surfactant molecule in the hydrophilic region. This micellar model — without invoking any further growth — is shown to explain the data for a wide range of concentrations at ambient temperature. Information about intermicellar interactions is obtained by analyzing the data using Baxter's sticky hard-sphere model, which assumes a square-well attractive potential between the micelles. This model is found to provide a qualitative interpretation of the temperature dependence of the data. However, important differences are noted for low momentum transfers. Some drawbacks of the model for characterizing the entire set of scattering data are brought out and discussed.

PACS number(s): 61.12.Ex, 61.25.Hq, 64.70.Fx

I. INTRODUCTION

Nonionic micellar solutions become cloudy on heating at a well defined temperature T_{CP} called the cloud point [1]. T_{CP} varies with surfactant volume fraction ϕ in the solution. Figure 1 shows the variation of T_{CP} with ϕ for a typical nonionic micellar solution (Triton X-100 – D_2O). The co-existence curve between high temperature and low temperature phases shows a lower consolute point (ϕ_c, T_c). It is well known that above the cloud point the solution separates into two phases — one rich and the other dilute in micellar concentration. Clouding phenomenon is analogous to the gas-liquid transition in pure liquids. For example, in both cases, the scattering cross section diverges in the low momentum transfer region as the sample temperature approaches T_{CP} [2–8]. It should be mentioned that there are important differences between the two phenomena. While the critical volume fraction is in the range of 15–30 % in the case of simple liquids, it is usually below 10% and can be as low as 1–2 % in micellar solutions [1]. The other important difference is that, in general, the co-existence curve is asymmetric about ϕ_c in micellar solutions while it is almost symmetric in the case of gas-liquid transition.

The gas-liquid transition in simple liquids is understood quite well from the point of view of interparticle interactions [9]. However, there is no satisfactory theory for explaining the clouding phenomena in micellar solutions. The statistical description of the micellar solution employs a single-component fluid model with micelles as the constituents [10]. The presence of water is introduced via an effective intermicellar potential energy $u(r)$. There are three contributions to $u(r)$: (i) the hard-sphere potential $u_{HS}(r)$; (ii) the van der Waals attractive potential $u_{vW}(r)$; and (iii) water mediated interaction $u_{WM}(r)$. It is believed that clouding arises due to the attractive intermicellar interaction $(u_a = u_{vW} + u_{WM})$, which become more important in the vicinity of T_{CP} [3].

Small-angle neutron-scattering (SANS) experiments on nonionic micellar solutions show that the scattering cross section $d\Sigma/d\Omega$ diverges in low Q $[Q = 4\pi \sin(\theta)/\lambda$, where θ is half the scattering angle and λ the wavelength] region as one approaches the cloud point [2–6]. This can, in principle, happen because of changes either in the particle form factor $P(Q)$ or in the interparticle structure factor $S(Q)$. Changes in $P(Q)$ would imply growth of micelles, and modifications in $S(Q)$ can be interpreted as arising from changes in intermicellar forces. The general consensus, however, is that micellar size does

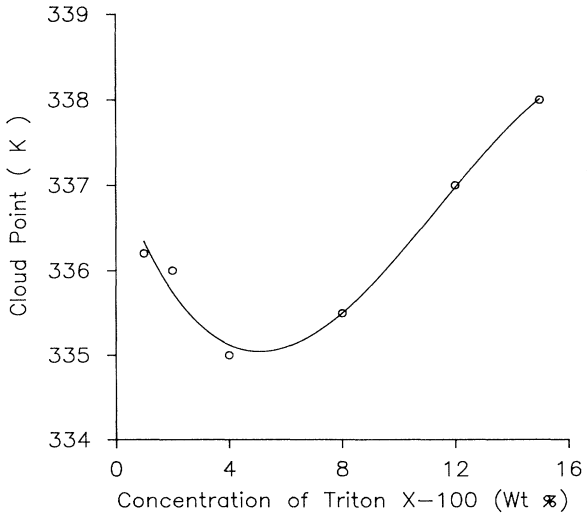

FIG. 1. Phase diagram of Triton X-100–D_2O.

not vary with temperature and that clouding arises because of changes in the intermicellar interaction potential [3,6,7,11]. As one approaches T_{CP}, the structure factor $S(Q)$ diverges at small Q values because of an increase in the attractive interaction between the micelles [3].

Reatto and Tau [12] have qualitatively explained the phase diagram of some nonionic micellar solutions by assuming Yukawa-type potentials for both the van der Waals part $u_{vW}(r)$ and the water mediated part $u_{WM}(r)$. Hayter and Zulauf [3] analyzed their SANS data on the n-octyl pentaoxyethylene glycol monoether (C_8E_5) solutions by modeling $(u_{vW}+u_{WM})$, again by a Yukawa-type attractive potential. This analysis, using the mean spherical approximation, gave somewhat large values (around $10K_BT$) for the potential depth near T_c. It has been argued in an earlier paper [4] that the potential depth should be about K_BT_c and the its large value obtained by Hayter and Zulauf is due to the use of the mean spherical approximation. We have carried out several studies [4,5,13] to examine the utility of Baxter's sticky hard-sphere model [14,15] for explaining the phase diagram and SANS data from nonionic micellar solutions. The sticky hard-sphere model, originally constructed [14] to show the gas-liquid transition in simple fluids, assumes that particles interact via a zero-range–infinite-depth attractive potential. This model is applied to micellar solutions by assuming that $(u_{vW} + u_{WM})$ can be approximated as an effective attractive square-well potential of depth u_0 and width Δ [4,13]. The attractive forces in micellar solutions have a short range [3] in comparison to the particle diameter σ, i.e., $\Delta/\sigma \approx 0.05$. This aspect makes Baxter's model a good candidate for modeling nonionic micellar solutions.

The structure factor $S(Q)$ and other thermodynamic quantities of Baxter's model can be expressed [15] in terms of a reduced parameter τ [defined in Eq. (12)]. Menon *et al.* [13] used this model to explain the neutron-scattering data from the C_8E_5 micellar solution for different temperatures at $\phi \approx \phi_c$. The dependence of $S(Q)$ for $Q \sim 0$ on ϕ, obtained from light scattering data for $T/T_c \leq 0.95$, as well as the phase diagram of C_8E_5 could be qualitatively explained by the model. This application indicated that below T_c the temperature dependence of τ can be approximately parametrized as $\tau/\tau_c = AT_c/T$, where A is a suitable constant and τ_c is the critical point value [14,15] of τ. To test this conclusion over a range of ϕ, Q, and T, and to see if the constant A is independent of surfactant concentration, Rao and co-workers [4,5] carried out SANS experiments on solutions of Triton X-100. These studies showed that the neutron cross sections for $\phi = 8\%$ and 15% could be fitted to the theoretical expressions reasonably well. The temperature dependence of τ could again be approximated as $\tau/\tau_c = AT_c/T$ for both concentrations; however, the constant A was different in the two cases. This observation was a bit surprising since the constant A is mainly decided by the interparticle potential (see the relation between τ and T quoted above) and hence should not change with ϕ if the model is robust. All these conclusions were, however, based on SANS data for $Q > 0.02$ Å^{-1}. Moreover, in these analyses, it was assumed that Triton X-100 micelles are spherical and have a uniform scattering length density. These assumptions are not quite valid as there are some reports [16] which suggest that micelles are oblate spheroids. Also, Triton X-100 micelles are expected to contain a significant amount of water in their hydrophilic region [16].

In view of the above, we have now carried out extensive measurements on Triton X-100 solutions. As compared to the lower limit of 0.02 Å^{-1} in earlier experiments, the Q range in the present experiments extends down to 0.006 Å^{-1}. Measurements have been made for several surfactant concentrations both above and below ϕ_c. This is particularly important as all our earlier SANS experiments have been confined to the region $\phi \geq \phi_c$. Baxter's model [14] shows that while $S(0)$, which is proportional to the compressibility of the one component fluid, diverges on the spinodal line in the region for $\phi \geq \phi_c$, it is finite for $\phi \leq \phi_c$. Thus the low concentration data are important to test the range of applicability of the model. For each concentration, measurements were made at several temperatures between room temperature and cloud point. The paper is organized as follows. Section II gives the experimental details. The relevant expressions for scattering laws are given in Sec. III. The results are discussed in Sec. IV. Finally, Sec. V gives a summary.

II. EXPERIMENTAL DETAILS

Triton X-100 (isooctylphenoxy polyethoxy ethanol) containing an average of 10 oxyethylene units per molecule was bought from Aldrich and used without further purification. The D_2O for SANS experiments was supplied by the Argonne National Laboratory. The micellar solutions were prepared in D_2O since the contrast between the micelles and the solvent in neutron experiments is better with D_2O than with H_2O. SANS experiments were performed at the Intense Pulsed Neutron Source at Argonne National Laboratory, Argonne, IL, using the small-angle diffractometer [17]. Measurements were made for surfactant concentrations of ϕ = 1, 2, 4, 8, 12, and 15% by weight. The cloud point temperatures for each of the samples were measured before starting the SANS experiments and they were, respectively, 336.5, 336, 335, 335.5, 337, and 338 K for the six surfactant concentrations. These temperatures are shown in Fig. 1 by open circles. The solid line in Fig. 1 is a guide to the eye. It may be noted that the cloud points for Triton X-100–D_2O solutions are somewhat lower than those for Triton X-100–H_2O solutions [18]. SANS data were recorded for about six temperatures between the ambient temperature (295 K) and the clouding temperature for each sample, the temperature intervals being smaller in the vicinity of T_{CP}. The concentration and temperature values corresponding to the experiments are indicated (together with the phase diagram) in Fig 2.

For SANS experiments, sample solutions were held in standard suprasil cells with a path length of 0.2 cm. The sample holder, wrapped in aluminum foil, resides inside a metallic cavity in a heating chamber with temperature control. The temperature of the sample is obtained as

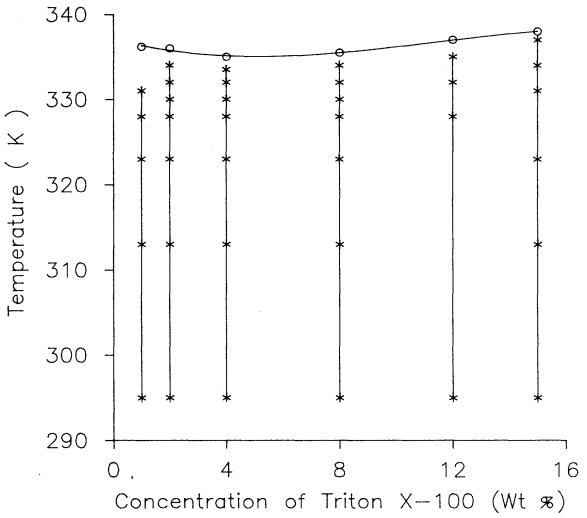

FIG. 2. Concentration and temperature space for Triton X-100–D_2O over which SANS experiments are reported in this paper. Crosses indicate the concentrations and temperatures corresponding to various measurements. Open circles represent the cloud points of the Triton X-100–D_2O solutions.

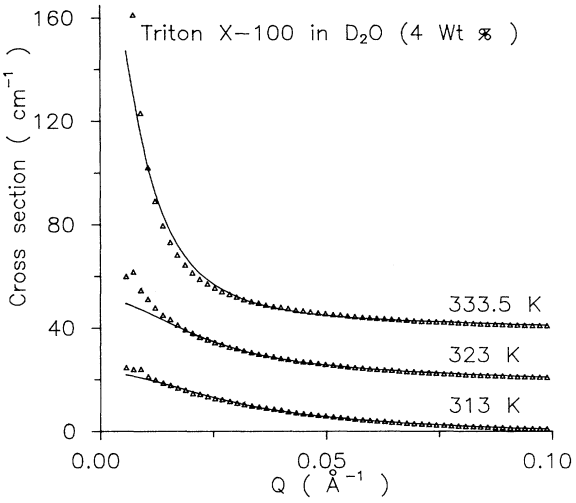

FIG. 4. SANS data from the 4% Triton X-100 solution at different temperatures. To avoid over crowding, data at $T = 295$, 328, 330, and 332 K are not shown here. Scattering cross section in the low Q region diverges as the cloud point T_{CP} (335 K) is approached. Solid lines are calculated curves.

that of the metal block at a point very near to the sample holder. To attain the set temperature, the sample was kept in the heating chamber for about an hour before starting the experiment. The aluminum foil around the sample holder ensures uniformity of temperature. Further, it was ensured that the detector counts the scattered neutrons only if the chamber temperature is between $(T_s - 1)$ and $(T_s + 0.5)$ K where T_s is the set temperature.

The measured distributions were corrected for monitor counts, detector efficiency, empty cell background, and the sample transmission. The data were then normalized to absolute cross-section units using standard procedures [17], and processed to obtain the differential scattering cross section $d\Sigma/d\Omega$ as a function of the magnitude of the scattering vector Q. Figures 3–6 show the typical data. As seen in Fig. 3, which shows the effect of surfactant concentration on $d\Sigma/d\Omega$ at 295 K, SANS distributions develop a correlation peak at $Q \sim 0.04$ Å^{-1} and this peak shifts to larger Q with increase in ϕ. Figures 4–6 show the effect of temperature on $d\Sigma/d\Omega$ for $\phi = 0.04$, 0.08, and 0.15, respectively. Data for $\phi = 0.01$, 0.02, and 0.12 are similar. To avoid crowding, data for only three

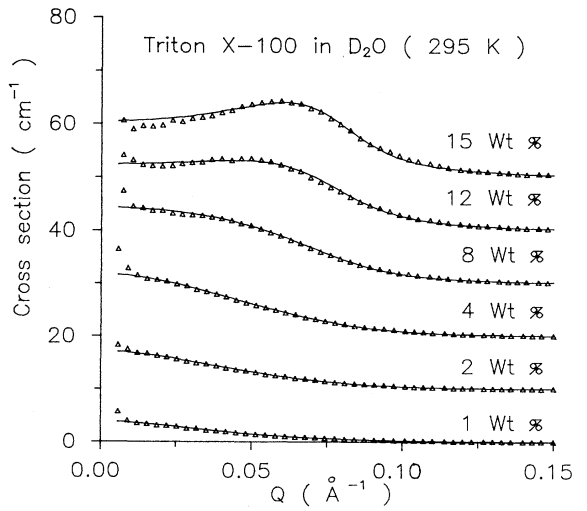

FIG. 3. SANS data at 295 K for varying concentrations of Triton X-100. Solid lines are calculated curves.

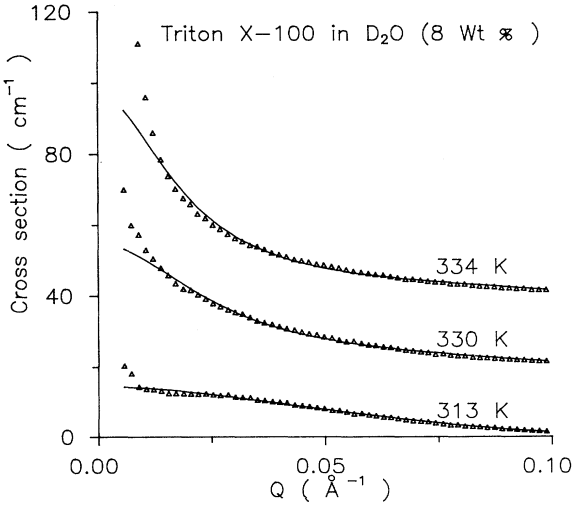

FIG. 5. SANS data from the 8% Triton X-100 solution at different temperatures. To avoid over crowding, data at $T = 295$, 323, 328, and 332 K are not shown here. The scattering cross section in the low Q region diverges as the cloud point T_{CP} (333.5 K) is approached. Solid lines are calculated curves.

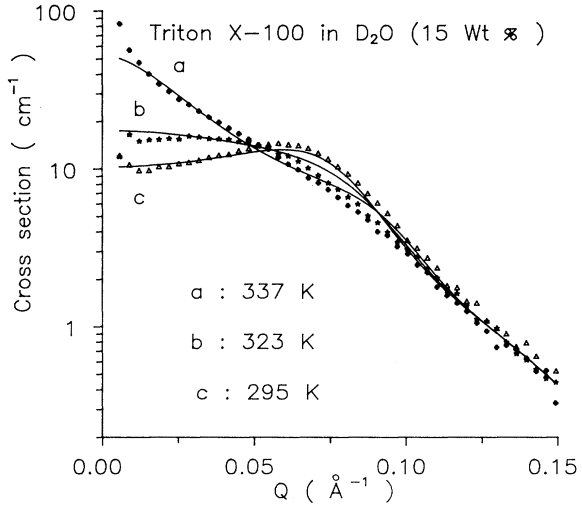

FIG. 6. SANS data from the 15% Triton X-100 solution at different temperatures. To avoid over crowding, data at $T = 313$, 331, and 334 K are not shown here. Scattering cross-section in the low-Q region diverges as the cloud point T_{CP} (338 K) is approached. The large-Q data are independent of temperature. Solid lines are calculated curves.

temperatures have been shown in Figs. 4–6. It is seen that, irrespective of the concentration, $d\Sigma/d\Omega$ in the low Q region diverges as T_{CP} is approached. However, large Q (> 0.1 Å^{-1}) cross sections are found to be independent of temperature within experimental errors. This is seen more clearly in Fig. 6, where $d\Sigma/d\Omega$ is plotted on a logarithmic scale. Again, for the sake of clarity, data corresponding to alternate Q values are only shown in this figure.

III. THEORETICAL EXPRESSIONS

For a system of monodisperse ellipsoidal micelles, the coherent differential scattering cross section can be expressed as [19–21]

$$\frac{d\Sigma}{d\Omega} = nP(Q)S(Q), \tag{1}$$

where n is the number density of micelles, $P(Q)$ is the single particle form factor, and $S(Q)$ is the structure factor. The incoherent scattering from the surfactant and the solvent contributes to a negligibly small background in the Q region of the experiments. $P(Q)$ for a two shell ellipsoid of revolution, with semi-axes $a_1 = b_1 \neq c_1$ for the core and $a_2 = b_2 \neq c_2$ for the outer shell, is given by [21]

$$P(Q) = \int_0^1 [V_1(\rho_1 - \rho_2)F_1(Q,\mu) + V_2(\rho_2 - \rho_3)F_2(Q,\mu)]^2 d\mu \tag{2}$$

$$F_i(Q,\mu) = \frac{3}{w_i^3}[\sin(w_i) - w_i\cos(w_i)] , \tag{3}$$

$$w_i = Q[c_i^2\mu^2 + a_i^2(1-\mu^2)]^{1/2} , \; i = 1,2 , \tag{4}$$

where μ is the cosine of the angle between the axis of revolution and Q. The volume of the core is V_1 and the total volume is V_2. The scattering length densities of the core, outer shell and solvent are ρ_1, ρ_2, and ρ_3, respectively. In the approximation that the center of mass and angular correlations of the micelles can be decoupled, the structure factor $S(Q)$ for an isotropic system has the expression

$$S(Q) = 1 + f(Q)n\int \exp(i\mathbf{Q}\cdot\mathbf{r})[g(r) - 1]d\mathbf{r} , \tag{5}$$

where $g(r)$ is the pair distribution function and

$$f(Q) = P(Q)^{-1}\left(\int_0^1 [V_1(\rho_1 - \rho_2)F_1(Q,\mu) + V_2(\rho_2 - \rho_3)F_2(Q,\mu)]d\mu \right)^2 . \tag{6}$$

The weighting factor $f(Q)$, which equals one for a spherical micelle, tends to unity as Q approaches zero.

In the following analysis, $S(Q)$ is calculated by approximating the ellipsoid to an equivalent sphere of diameter $\sigma = (a_2^2 c_2)^{1/3}$ and then using Baxter's sticky hard-sphere model [14]. Menon *et al.* [15] have shown that this model depicts the micellar system as a collection of (spherical) particles interacting via a thin attractive square-well potential of depth u_0 (< 0) and width Δ. The basic results of the model can be derived as the lowest order solution, in the parameter $\epsilon = \Delta/(\sigma + \Delta)$, to the Ornstein-Zernike equation and Percus-Yevick closure relation [15]. The expression for the structure factor is given by

$$S^{-1}(Q) = A^2(Q) + B^2(Q) \tag{7}$$

$$A(Q) = 1 + 12\eta\left(\alpha\frac{s(k) - kc(k)}{k^3} + \beta\frac{1 - c(k)}{k^2} - \frac{\lambda}{12}\frac{s(k)}{k} \right) \tag{8}$$

$$B(Q) = 12\eta\left(\alpha\left[\frac{1}{2k} - \frac{s(k)}{k^2} + \frac{1 - c(k)}{k^3}\right] + \beta\left[\frac{1}{k} - \frac{s(k)}{k^2}\right] - \frac{\lambda}{12}\frac{1 - c(k)}{k} \right), \tag{9}$$

where $s(k) \equiv \sin(k)$, $c(k) \equiv \cos(k)$, $k \equiv Q(\sigma + \Delta)$, and

$$\alpha = \frac{1 + 2\eta - \mu'}{(1-\eta)^2} , \; \beta = \frac{-3\eta + \mu'}{2(1-\eta)^2} , \; \mu' = \lambda'\eta(1-\eta) \tag{10}$$

$$\lambda' = \frac{6}{\eta}[\delta - (\delta^2 - \nu)^{1/2}] , \; \delta = \tau + \frac{\eta}{1-\eta} , \quad \nu = \eta\frac{1 + \eta/2}{3(1-\eta)^2} . \tag{11}$$

The parameter $\eta = \pi n(\sigma + \Delta)^3/6$ is the particle "volume fraction" which includes the potential width. τ is related to the potential parameters (u_0, Δ, σ) and temperature T as

$$\tau = \frac{\sigma + \Delta}{12\Delta} \exp(u_0/K_B T), \tag{12}$$

where K_B is the Boltzmann constant. In the present application, the particle diameter σ ($\approx$ 75 Å) is much larger than the potential width Δ ($\sim$ 2 Å) [3] and so η has been taken as the true volume fraction.

IV. RESULTS AND DISCUSSION

We note that, at the ambient temperature, the SANS distributions decrease monotonically for low surfactant concentrations, but show a well defined peak for higher concentrations (Fig. 3). As already mentioned, the measured $d\Sigma/d\Omega$ depends on the product of the form factor $P(Q)$ and the structure factor $S(Q)$. The peak in the measured distribution arises because of a corresponding peak in $S(Q)$. At low concentrations, micelles are far apart and interparticle interference effects are negligible, except at very low Q values. Therefore, the effect of $S(Q)$ becomes important only at high concentrations where one sees a well defined peak in $d\Sigma/d\Omega$. The shift in the peak to larger Q values is due to the reduction in the intermicellar distances with increase in surfactant concentration. In the following, we first analyze the data for $\phi = 0.01$ where the measured distribution is largely decided by the particle form factor $P(Q)$. Thus these data are most conveniently used to obtain the size and shape of micelles.

A. Size and shape of Triton X-100 micelle

The critical micelle concentration for Triton X-100 is about $0.35mM$ and in the concentration range of our experiments, the number of free monomers will be negligible compared to those in the micelles. Determination of the size and shape of triton X-100 micelles has been the subject of several investigations [16,22–25]. Most of these studies show that the molecular weight of the micelle is around 90 000 which corresponds to an aggregation number of 145 [22–24]. However, regarding the shape of the micelle, some studies suggest that the micelles are spherical [22–24] while others [16,25] argue that micelles are oblate ellipsoids. This difference arises partly due to the omission, in some of the analyses, of the water of hydration in the hydrophilic region. It may be noted that the central core of the micelle consists of hydrophobic alkyl chains and the outer shell is made up of hydrophilic oxyethylene chains. The lengths of the hydrophobic and hydrophilic parts of Triton X-100 molecule are comparable. Thus there could be significant amount of water in the outer shell [16,26–28].

Robson and Dennis [16] argued that the core of the micelle should be oblate in shape ($a_1 = b_1 = 35$ Å, $c_1 = 10$ Å) since one cannot pack 145 octyl phenyl groups in a sphere having a radius of 10 Å (equal to the length of the octyl phenyl group). An oblate shape (instead of a prolate shape) has been chosen from considerations of intrinsic viscosity of the solutions. They further argued that the length of oxyethylene chain is 17 Å and suggested that the overall micellar shape is oblate having semiaxes $a_2 = b_2 = 52$ Å and $c_2 = 27$ Å. Then, from density considerations, they concluded that there are about 40 molecules of water per surfactant molecule in the hydrophilic region. This micellar model is, however, based on some unknown parameters: the length of the oxyethylene chain, its disposition within the hydrophilic layer, and the overall density of the hydrophilic region. It is not straightforward to obtain the outer dimensions of the micelle as the length of polyoxyethylene chain is not known — it depends on the chain conformation in the micelle [16]. In view of this, we have obtained the dimensions of Triton X-100 micelles from SANS experiments which are sensitive to the overall dimension. SANS is also sensitive to the presence of D_2O in the hydrophilic region, which results in an increase in the scattering length density of that region.

We note that an aggregation number of 145 would give an interparticle distance of about 250 Å for $\phi = 0.01$ solution and the structure factor $S(Q)$ is expected to peak around $Q \approx 0.025$ Å^{-1}. Thus the small Q region cannot be used for getting information on the shape of the micelle. We have thus used data corresponding to $Q > 0.03$ Å^{-1} for obtaining the structural parameters of the micelle. The analysis involved comparing the calculated $d\Sigma/d\Omega$ with the measured cross sections (Fig. 7). The micellar model used in the analysis is that of Robson and Dennis [16]. Following them, we assume that the micelle is an oblate ellipsoid consisting of an inner core and an outer shell with $a_1 = b_1 = 35$ Å and

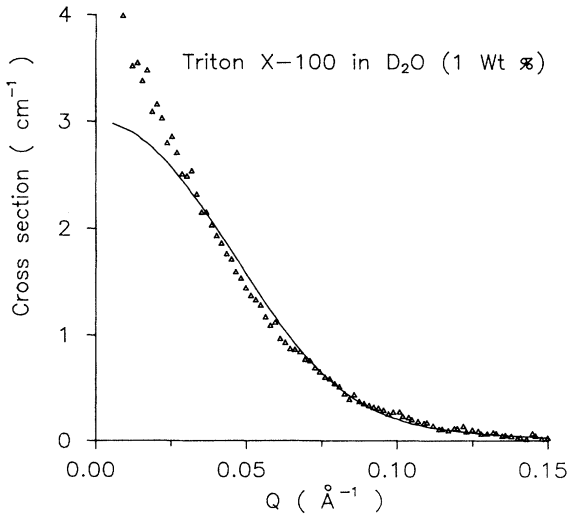

FIG. 7. SANS data from 1% Triton X-100 solution at 295 K. The solid line is the fitted ($Q > 0.03$ Å^{-1}) single particle cross section which is determined by the structure of the micelle. Differences in the measured and calculated distributions for $Q < 0.03$ Å^{-1} arise because of interparticle interference effects.

$c_1 = 10$ Å. In the absence of intermicellar interference effects, the SANS distribution is given by Eq. (1) with $S(Q) = 1$. The dimensions of the outer shell $a_2 = b_2$ and c_2 were taken as fitting parameters. The scattering length density of the core $\rho_1(0.403 \times 10^{10}$ cm$^2)$ and the solvent $\rho_3(6.38 \times 10^{10}$ cm$^2)$ are known quantities. The parameter ρ_2 for the outer shell, which depends on the amount of hydration of the shell, also was varied in the analysis. Thus the data corresponding to $\phi = 0.01$ for $Q \geq 0.03$ Å^{-1} were fitted to Eq. (1) [with $S(Q) = 1$] with a_2, c_2, and ρ_2 as parameters. Results are shown in Fig. 7. The disagreement between the calculated and experimental curves for $Q < 0.03$ Å^{-1} is mainly due to the interparticle interference effects which have not been taken into account in the calculation. There exists also the possibility that a small fraction of the micelles are long and flexible and they contribute to the scattered intensity in the low Q region [29]. The present analysis yielded $a_2 = b_2 = 47.5$ Å and $c_2 = 22.5$ Å. Incorporating polydispersity in the parameter a_2 did not alter the fit shown in Fig. 7 significantly. Thus the dimension of the hydrophilic region is about 12.5 and not 17 Å as assumed by Robson and Dennis. The value of ρ_2 was found to be 3.9×10^{10} cm^2 which corresponds to about 20 water molecules per surfactant molecule [i.e., two water molecules (n_w) per oxyethylene unit] in the hydrophilic region of the micelle. This is in excellent agreement with the NMR studies of Beyer [27], where he found that there are about 2.0 to 2.2 water molecules per oxyethylene units in Triton X-100 micelles. Recent Raman scattering studies [28] on the $C_{10}E_5$ system also shows that $n_w \approx 1.4$ to 1.7. Robson and Dennis had estimated this number of D_2O molecules by assuming that the density of the outer shell of the micelle is same as that of polyethylene oxide which is approximately 1.13. Making such an assumption regarding density, the number of D_2O molecules in the hydrophilic region comes to 15, which is not very different from the number calculated from ρ_2. Thus the complete set of numbers, namely the minor and major axes and the number of D_2O molecules in the hydrophilic region, as derived by different methods, are entirely consistent. A possible picture which emerges from this is that the oxyethylene chains flex (bend) sufficiently to reduce the width of the hydrophilic layer and bring its density as near to its normal value as possible and that it has to take in only 20 D_2O molecules instead of 40. It seems that the higher value of n_w obtained by Robson and Dennis is because of the assumption that the oxyethylene chains are somewhat stretched out.

B. Effect of surfactant concentration

The effect of surfactant concentration on SANS distributions is shown in Fig. 3 for $T = 295$ K. The peak in $d\Sigma/d\Omega$ at high concentrations arises from intermicellar interference effects. With an increase in concentration, the interparticle distance decreases and the peak shifts to larger Q values. The data have been analyzed in terms of Eq. (1). For calculating $S(Q)$, particles were replaced by a sphere of equal volume and the formulas corresponding to Baxter's model were employed. Volume of the micelle was taken to be independent of concentration of Triton X-100. The solid lines in Fig. 3 are the fitted curves. τ values obtained from the fits are plotted in Fig. 8, which is discussed below. The micellar volume is about 2.12×10^5 Å and hence one gets, for example, a "particle" volume fraction $\eta = 0.21$ when $\phi = 0.15$. This is because of the fact that the micelle contains about 2900 molecules of water. If no water was trapped in the micelle, the values of η and ϕ would have been equal. It is seen that calculated distributions give the peak positions in $d\Sigma/d\Omega$ more or less correctly. Thus we conclude that the aggregation number 145 and the micellar shape parameters determined from the $\phi = 0.01$ data provide a consistent picture for all surfactant concentrations.

C. Effect of temperature

Baxter's model predicts a gas-liquid phase transition with a universal phase diagram in the τ-η plane with an upper consolute point given by $\tau_c = 0.097$ and $\eta_c = 0.12$ [14]. By assuming that the potential depth u_0 varies with temperature, this phase diagram can be transformed into one with a lower consolute critical point (T_c, η_c) in the T-η plane as in the case of nonionic micellar solutions [13]. The critical surfactant volume fraction for Triton X-100 is around 0.06 which yields a particle volume fraction 0.085. If the intermicellar interactions can be modeled in terms of a temperature dependent square-well potential, it would be possible to fit the measured scattering cross sections for all volume fractions by varying the parameter τ with temperature. The neutron cross-sections (Figs. 4–6) build up at low Q values as the temperature is increased. Therefore τ should decrease as the temperature is increased. Equation (12) shows that the potential depth u_0 must decrease with temperature to compensate the factor T^{-1} in the exponential function. The fits obtained for $\phi = 0.04$, 0.08, and 0.15 are shown by the

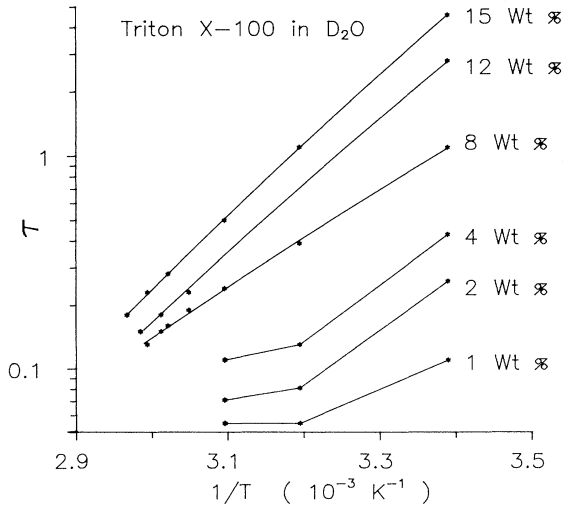

FIG. 8. Variation of interaction parameter τ with temperature for different concentrations of Triton X-100.

solid lines in Figs. 4–6. The interaction parameter τ is the only variable that has been adjusted to obtain these fits. The calculated values for all cases agree quite well for $Q > Q_0 \sim 0.01$ Å^{-1}. However, there are significant deviations for lower values of Q as seen in these figures. These observations suggest that spatial correlations up to a length scale of $2\pi/Q \approx 600$ Å $(= 8\sigma)$ are accounted for adequately by the model.

For each value of η, there is a lower limit to the value of τ in the single phase region pertaining to the neutron experiments. The limiting values are determined from the spinodal curve in the τ-η plane for Baxter's model [14]. Therefore, the parameter τ was restricted to be above the limiting values in obtaining the fits to neutron data. As mentioned earlier, Baxter's model has a drawback that the compressibility [and hence $S(0)$] does not diverge as one approaches the spinodal curve in the "gaseous" branch, that is for $\eta < \eta_c$. Therefore, for $\phi = 1\%$, 2%, and 4%, the build up of scattering cross sections is not completely accounted for by the model. These features were not evident from previous applications [4,5,13] of Baxter's model as they were restricted to higher values of the ϕ and Q range. The values of τ (on a logarithmic scale) derived for different ϕ are plotted as a function of T^{-1} in Fig. 8. For lower concentrations ($\phi = 1\%$, 2%, 4%), τ values are shown only for low temperatures (295, 313, and 323 K) because the limiting values were reached by about 323 K. Thus high temperature data for low surfactant concentrations are not accountable using Baxter's model. It is interesting to note that the behavior of $\ln(\tau)$ vs T^{-1} curves for $\phi < \phi_c$ is significantly different from that for $\phi > \phi_c$. This also indicates that Baxter's model may not be appropriate for characterizing the Triton X-100 solution for $\phi < \phi_c$.

Because of an improved model for $P(Q)$ used in the present analysis, we believe that the temperature dependence of τ for $\phi = 8\%$ and 15% obtained now is better than what was deduced in our earlier work [4,5]. As against the earlier derived relation $\tau/\tau_c = AT_c/T$, we find that an expression of the type $\ln(\tau) = B/T + C$ provides a better relationship between τ and T. We also note that (see Fig. 8) the constant B has more or less the same magnitude for all values of ϕ, especially for $\phi > \phi_c$. Then Eq. (12), which relates τ and u_0 implies that u_0 varies linearly with temperature. Assuming $\Delta \sim 2.5$ Å (size of the water molecule) [3,4], from Eq. (12) we get for $\phi = 0.08$ solution, $u_0/K_BT \sim -0.9$, -2.6, and -2.9, respectively, for $T = 295$, 328, and 334 K. In short, we find that the potential depth u_0 is comparable to K_BT_c near critical concentration and not of the order of $10K_BT_c$ as obtained by Hayter and Zulauf [3]. Contrary to what was expected, we find that the values of u_0 depend on surfactant concentration ϕ since the absolute values of τ vary with ϕ. Perhaps this is due to the adaptation of a single component fluid model for the micellar solution and the over simplified interaction potential employed in Baxter's model. In addition, it has been assumed that there is no micellar growth with temperature.

A better description of long range correlations may be obtained with a more detailed representation of intermicellar potential [10,12]. However, this would require a numerical calculation of $S(Q)$ using the Ornstein-Zernike equation. Whether such a model, with a minimal set of parameters, can describe the temperature dependence of low Q data for all concentrations is being investigated.

V. SUMMARY

This paper reports measurements of neutron cross sections from the micellar solution of Triton X-100 in D_2O over a wide range of surfactant concentrations and temperatures in the single phase region. Measurements have covered Q ranges from 0.006 to 0.2 Å^{-1}. The analysis of data for dilute solutions has yielded an oblate ellipsoidal model of the micelle with semi-axes of 47.5 and 22.5 Å. That is, we find that the polyoxyethylene chains are not as extended as was assumed in earlier studies [16]. It is also found that the hydrophilic shell of the micelle has about 20 water molecules per surfactant molecule. This micellar model is found to explain scattering cross sections at ambient temperature for a wide range of surfactant concentrations up to 15%. That is, the peak in the structure factor arising out of the intermicellar correlations is found to be in accordance with this model. Baxter's sticky hard-sphere model, which assumes a thin attractive square-well potential for intermicellar interactions, is found to provide a qualitative interpretation of the temperature dependence of cross sections in the Q range above 0.01 Å^{-1}. We find that the interaction potential u_0 varies linearly with temperature and has a value of about $3K_BT_c$ near T_c. Significant deviations between the measurements and predictions of the above model have been found for $Q < 0.01$ Å^{-1}. These differences indicate that the model does not account for spatial correlations in micellar solutions over longer length scales (greater than 8σ). Further, the picture depicting Triton X-100 micelles as a single component fluid interacting via a short ranged (temperature dependent) attractive potential is found to be not completely consistent since the derived potential parameter (τ) depends on the surfactant concentration also. Thus it is concluded that a complete characterization of the temperature dependence of low-Q neutron data needs finer details of intermicellar interactions.

[1] V. Degiorgio, in *Physics of Amphiphiles: Micelles, Vesicles and Microemulsions,* edited by V. Degiorgio and M. Corti (North-Holland, Amsterdam, 1985).

[2] L. J. Magid, R. Triolo, and J. S. Johnson, J. Phys. Chem. **88**, 5730 (1984).

[3] J. B. Hayter and M. Zulauf, Colloid. Polym. Sci. **260**, 1023 (1982).

[4] K. S. Rao, P. S. Goyal, B. A. Dassanacharya, V. K. Kelkar, C. Manohar, and S. V. G. Menon, Pramana J. Phys. **37**, 311 (1991).

[5] K. S. Rao, P. S. Goyal, B. A. Dassanacharya, S. V. G. Menon, V. K. Kelkar, C. Manohar, and B. K. Mishra, Physica **B174**, 170 (1991).

[6] J. Penfold, E. Staples, and P. G. Cummins, Adv. Colloid.

Interface Sci. **34**, 451 (1991).
[7] M. Corti and V. Degiorgio, Phys. Rev. Lett. **55**, 2005 (1985).
[8] M. Corti, C. Minero, and V. Degiorgio, J. Phys. Chem. **88**, 309 (1984).
[9] H. E. Stanley, *Introduction to Phase Transitions and Critical Phenomena* (Oxford University Press, Oxford, 1971).
[10] L. Reatto, in *Surfactants in Solution*, edited by K. L. Mittal (Plenum, New York, 1989), Vol. 7.
[11] V. Degiorgio and R. Piazza, Prog. Colloid. Poly. Sci. **73**, 76 (1987).
[12] L. Reatto and M. Tau, Chem. Phys. Lett. **108**, 292 (1984).
[13] S. V. G. Menon, V. K. Kelkar, and C. Manohar, Phys. Rev. A **43**, 1130 (1991).
[14] R. J. Baxter, J. Chem. Phys. **49**, 2770 (1968).
[15] S. V. G. Menon, C. Manohar, and K. S. Rao, J. Chem. Phys. **95**, 9186 (1991). Baxter's original derivation implicitly assumed a form $f(r) = -1+\delta(r-\sigma)\sigma/12\tau$ for the Mayer function which characterizes a zero-range–infinite-depth interparticle potential.
[16] R. J. Robson and E. A. Dennis, J. Phys. Chem. **81**, 1075 (1977).
[17] J. E. Epperson, J. M. Carpenter, R. K. Crawford, P. Thiyagarajan, T. E. Klippert, and D. G. Wozniaik (unpublished).
[18] A. S. Sadaghiania and A. Khan, J. Colloid. Interface Sci. **144**, 191 (1991).
[19] J. B. Hayter and J. Penfold, Mol. Phys. **42**, 109 (1981).
[20] S. H. Chen and T. L. Lin, in *Methods of Experimental Physics* (Academic Press, New York, 1987), Vol. 23B, p. 489.
[21] S. S. Berr, J. Phys. Chem. **91**, 4760 (1991).
[22] W. Brown, R. Rydman, J. V. Stam, M. Almgren, and G. Svensk, J. Phys. Chem. **93**, 2512 (1989).
[23] L. M. Kushner and W. D. Hubbard, J. Phys. Chem. **58**, 1163 (1954).
[24] S. Yedgar, Y. Barenholz, and V. G. Cooper, Biochem. Biophys. Acta. **363**, 98 (1974).
[25] A. K. Wright, J. Colloid. Interface. Sci. **55**, 109 (1976).
[26] V. Degiorgio, M. Corti, R. Piazza, L. Cantu', and A. R. Rennie, Colloid. Poly. Sci. **269**, 501 (1991).
[27] K. Beyer, J. Colloid. Interface Sci. **86**, 73 (1982).
[28] N. Micali, C. Vasi, F. Mallamace, M. Corti, and V. Degiorgio, Phys. Rev. E **48**, 3661 (1993).
[29] J. C. Eriksson and S. Ljunggren, Langmuir **6**, 895 (1990).